Personalizing Risk Assessment of Atrial Fibrillation and COVID Thrombophilia using Noninvasive Ultrasound Detection of Microthrombi

Saksham Saksena; Mentor: Dr. Sandeep Rajan (Vanderbilt University Medical Center)

Background

Cardiovascular Diseases are the Top Killers in US. This study focused on atrial fibrillation and COVID-19 related thrombophilia. Currently, CHADS2 scores are used to evaluate risk of stroke from Atrial Fibrillation, in order to determine treatment by anticoagulants. However, this does not allow for personalization, potentially leading to erroneous treatment. Proposed tests for COVID-19 Thrombophilia are new and speculative, with uncertain efficacy.

Microthrombi (30 – 70 μm) are much greater in size than normal blood cells (4 – 12 μm) (as shown in Table 1). Discrimination of such differential size by continuous scanning of a blood vessel offers an attractive new risk assessment for these grave maladies of mankind.

Cell Type	Size Range (μm)
White Blood Cell (WBC)	6-12
Red Blood Cell (WBC)	4-8
Microthrombi (μT)	30-70

Table 1: Size Comparison of Cells

Methods

Ultrasound Phantom and Yeast Samples

In this study, yeast and yeast clusters of different sizes were used as a surrogate for circulating cells to create a proof of principle for noninvasive detection via ultrasound of Microthrombi (μT) as an personalize risk assessment modality for Atrial Fibrillation and COVID thrombophilia. For this study, a closed circulation system with an Ultrasound Phantom (UP) with wall-less vessels was created using the following steps (adapted from [1]) A vessel tube was placed in a cartridge. 5.5% agar solution heated to 90°C and cooled to 55°C, mimicking soft tissue, was poured into the cartridge, and refrigerated at 4°C for 12 hours to solidify. The vessel tube was carefully removed and intravenous (IV) tube connectors were fastened to the two ends of the wall-less cavity in the solidified agar. IV tubing, an 250ml 0.9% sodium chloride, normal saline (NS), IV bag, and a Braun Vista infusion pump were connected to this system, as seen in figure 1 below.

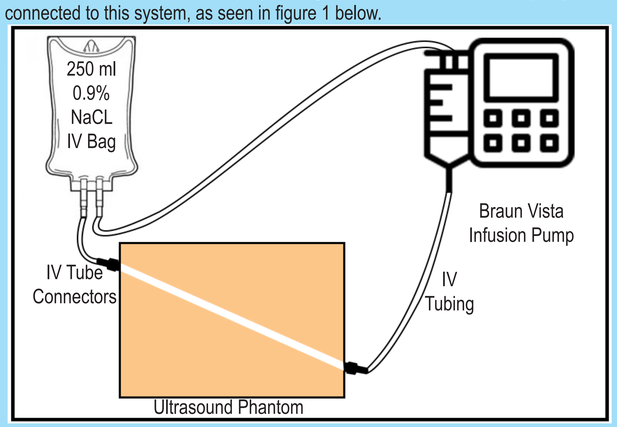

Figure 1: Closed Circulatory Circuit (CCC) Set-up

To such IV bags, 25ml of respective sample solutions, as described below, were injected. This closed circulatory circuit (CCC) represented the systemic circulation of the body with the Infusion Pump, mimicking the heart, was set at infusion rate of 800ml/hr. Each sample added to the IV bag was passed through our CCC, changing the tubing and flushing the UP with 25ml of NS between each sample. Doppler ultrasound was performed over UP for 10-minute duration using a 2-MHZ probe of GE LOGIQ e machine. Screenshots of the screen were taken every 15 seconds.

Sample Descriptions: Instant yeast (Baker's Corner distributed by Aldi Inc. Batavia, IL) was used. 0.7g was added to 100ml H2O at 37°C. Four yeast samples were prepared (first three samples shown in Figure 2a). In the first sample (Figure 2b), yeast was only mixed with water to represent normal blood cells (5 μm). The second yeast sample (Figure 2c) was incubated with sugar (9g per 100ml) and starch (9g per 100ml) for 1 minute to represent Small μT (20-30 μm). After 1 minute, for every 24ml sample solution, 1ml 4.8 mmol sodium fluoride (NaF) solution was added to block enolase, hence arresting further yeast division by blocking glucose metabolism. The third sample (Figure 2d) was incubated with starch and sugar (same as sample 2) for 15 minutes (adding NaF in same proportions at the end) to represent Large μT (60-100 μm). A fourth yeast sample was made by mixing the other 3 samples in 8:1:1 proportion (mimicking circulating blood in cardiovascular disease). Fifth sample had NS only.

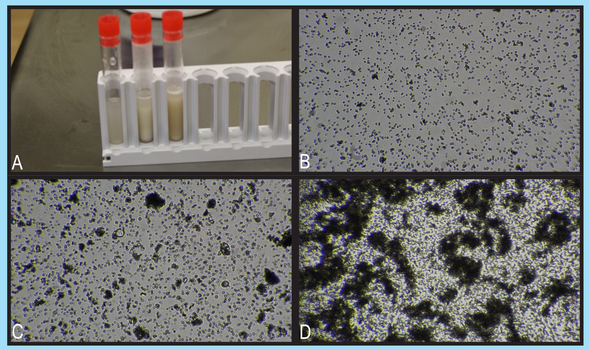

Figure 2: A - From left to right: Sample 1, Sample 2, and Sample 3. Sample 4 was made by mixing portions of these three. B - Sample 1 (40x Microscope View). C - Sample 2 (40x Microscope View). D - Sample 3 (40x Microscope View).

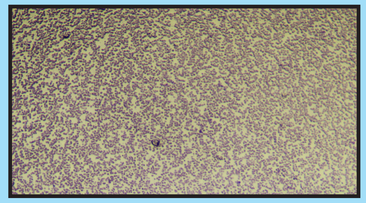

Figure 3: Blood Smear at 40x Microscope View. RBCs are more crowded but comparable in size to the surrogate samples.

Convolutional Neural Network

A real-time ultrasonography would require extensive time expense and errors due to visual fatigue even by experienced radiologists. Hence, machine learning strategies were used for automation and potentially improved accuracy. A Convolutional Neural Networks with binary classification were built to distinguish between Samples 2, 3, & 5. The screenshots of the ultrasound data were processed in the manner shown in Figure 4. First, the 40 screenshots obtained for Sample 2, 3, and 5 each needed to be pre-processed to prepare data to be inputed into the Neural Network. The screenshots obtained from the Ultrasound Machine were stored as 1 frame videos (in WMV format). For the Neural Network, JPG inputs were preferred. To derive JPG pictures for each screenshoted ultrasound data, the following steps were taken:

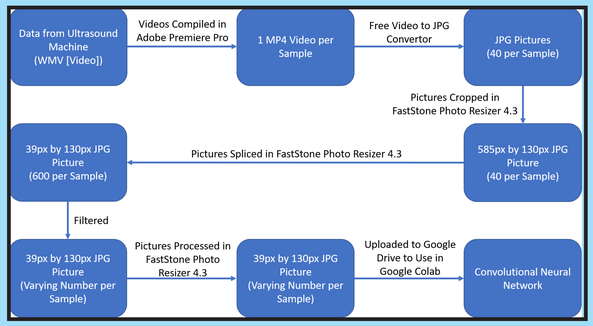

Figure 4: Diagram of the steps taken to process the Screenshots of the Ultrasound Data

For the Convolutional Neural Network (CNN) models, Python code, with Keras, was used on the Google Colaboratory platform. The processed data was uploaded to Google Drive. Google Drive was mounted in the model in order to access the data. The data was appended, shuffled, and converted into a numpy array. The numpy array was inputed into CNNs. 60 models each were tested for 3 different distinctions: Large μT (Sample 3) vs. Normal Saline (Sample 5) (A), Small μT (Sample 2) vs. Normal Saline (B), and Large μT vs. Small μT (C). The models exhaustively tested 1 or 2 Convolutional Blocks with activation 'relu'; 2, 4, 8, 16, or 32 nodes (the number of filters in a convolutional block); and 1 to 6 epochs. The first model (1) for each distinction has 2 convolutional blocks, 32 nodes, and 6 epochs with consecutive models decreasing first in epochs, then in nodes, and finally in layers. After each convolutional block, there is a dropout layer with dropout chance 0.3. In each model, there is a flatten and 2 dense layers.

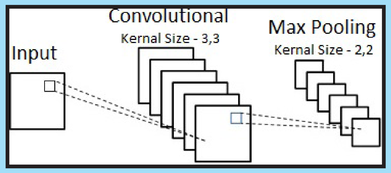

Figure 5: Diagram of Layers in Convolutional Block (adapted from [2])

The study author evaluated (with batch checking by mentor) a shortened set of the full data used to train the CNN. Results of this human evaluation were compared to the most accuracte CNN model.

Results

Doppler signals from the third sample of yeast, representing Large μT surrogates, varied significantly from that of the first, second, and fifth samples in terms of intensity. This also allowed distinction between Large μT from other particles in the fourth sample. Sample 2 could not be distinguished from sample 1.

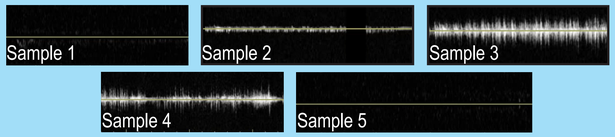

Figure 6: Sample 1 - Normal Blood Cells; Sample 2 - Small μT; Sample 3 - Large μT; Sample 4 - 8:1:1 mix of the previous 3 samples; Sample 5 - Normal Saline, only.

The Convolutional Neural Network, made to improve accuracy and automate the process, proved greater accuracy. The most accurate models for each distinction were A2, B31, and C7 respectively. Overall, A2 was the most accurate. The sensitivities and specificities for each of the models were also calculated. After training for 4 epochs, the model had a training accuracy of 0.9856 and a validation accuracy of 0.9863, as shown by the Training & Validation Accuracy curve in Figure 8. Four other models were also trained, their accuracy and loss are depicted in Table 2.

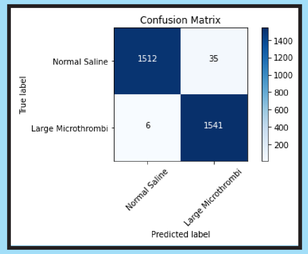

Figure 7: Confusion Matrix for Model A2 (Large μT vs. Normal Saline)

Model	A2	B31	C7
Training Accuracy	0.9921	0.6670	0.9571
Validation Accuracy	0.9731	0.6087	0.9636
Test Accuracy	0.9817	0.6801	0.9598
Sensitivity	0.9964	0.5553	0.9993
Specificity	0.9774	0.8199	0.9016

Table 2: Comparison of Accuracies, Sensitivity, and Specificity of the top model of each distinction

Human evaluation of the shortened data yielded a lower accuracy of 0.9374. Its Sensitivity, the chance that a predicted Large μT signal is true positive, was 0.9604; its Specificity, the chance that a predicted Normal Saline signal is true negative, was 0.9143. Both of these measures were also lower than similar measures for model A2.

Discussion

In this study, the energy in the fluid is evenly spread throughout the volume. Modifying the basic equation for kinetic energy, $E / V = 1/2\ \rho\ v^2$ is derived, where E is energy, V is volume, ρ is density, and v is velocity. Therefore, a higher density particle, i.e. yeast clusters acting as surrogates for Large μT, will have lower velocity. Since the flow rate remains constant, the velocity of the normal saline surrounding the clusters has to rise, as the energy required to achieve the flow rate rises. This directly corresponds to higher intensities seen in Sample 3. Similar mechanisms are found in the human body. Hence, a similar phenomena can be expected in the human body.

Interestingly, while the other 2 classifications host incredible accuracy, distinction between Small μT surrogates and Normal Saline had poor accuracy, suggesting the ultrasound sensor used does not have a large enough frequency to effectively distinguish between Small Microthrombi and Normal Blood.

The CNN models were more accurate than the human evaluation. Proposed factors behind this were the limitations of eyes and low screen contrast preventing detection of finer details that could aid in detection and visual fatigue.

Thus, this provides a proof of principle demonstration, through the CCC system, suggesting that large μT can be detected through real-time Doppler ultrasound over carotid artery. Using such an approach for diagnosis, ultrasound detection of microthrombi could result in a faster and more effective risk assessment of Atrial Fibrillation and COVID-19 thrombophilia.

The universality, non-invasive nature, automation, and high accuracy of this proposed methodology makes it ideal for a preliminary screening test. If particles are detected, confirmatory tests to determine exact cause of disease can be conducted later. This test will reduce the number of tests for the general public as only patients test positive for Cardiovascular Diseases will require further screening. This would make the screening process easier and enable greater reach without any pain or radiation exposure.

Future Work

Further trials need to be conducted with the use of cell lines, rather than yeast surrogates, leading up to a clinical trial. Trials will need to be conducted to determine what levels of microthrombi equate to certain treatments. To determine these guidelines, a group of patients for different disease should be screened using the methodology and clotting events observed, without any treatment. Experts can then determine thresholds for treatment for different diseases.

In this study, small μT signals were not able to be detected accurately. However, with an ultrasound sensor with higher frequency (in GHZ range), these smaller particles might also become detectable. This would further improve the accuracy of the methodology proposed in this study. Additionally, new breakthrough ultrasound technology can be used to create a wearable ultrasound sensor, allowing for remote (potentially at-home) testing.

References

1. Nikitichev DI, Barbura A, McPherson K, Mari JM, West SJ, Desjardins AE. Construction of 3-Dimensional Printed Ultrasound Phantoms With Wall-less Vessels. J UltrasoundMed 2016; 35:1333–1339.
2. Phung, & Rhee,. (2019). A High-Accuracy Model Average Ensemble of Convolutional Neural Networks for Classification of Cloud Image Patches on Small Datasets. Applied Sciences. 9. 4500. 10.3390/app9214500.

I would like to thank my mentor Dr. Sandeep Rajan, Associate Professor, Division of Hematology/Oncology Medical Director, Erlanger/Vanderbilt University Medical Center